MATERIALS CHEMISTRY
FRONTIERS

REVIEW

View Article Online
View Journal | View Issue

Cite this: *Mater. Chem. Front.*, 2019, **3**, 2246

Utilization and prospects of electrochemiluminescence for characterization, sensing, imaging and devices

Zhen Zhang, †[a] Peiyao Du, †[ab] Guiqiang Pu,†[a] Liping Wei,[b] Yanxia Wu,[b] Jinna Guo[a] and Xiaoquan Lu *[ab]

Received 30th June 2019,
Accepted 5th September 2019

DOI: 10.1039/c9qm00426b

rsc.li/frontiers-materials

Electrochemiluminescence (ECL) involves the generation of species by an electrochemical stimulus to induce luminescence, representing a highlighted specific field over decades for various analytical applications. In this review, we have summarized the recent development of a large number of ECL luminophores, which can be categorized as single molecules, nanostructured materials, and heterocyclic compounds with AIE effects. Moreover, we discussed the applications of ECL in many fields, such as material characterization, sensing, imaging and devices. We firmly believe that this review will attract extensive attention.

1. Introduction

Electrochemiluminescence (ECL), proposed by Hercules and Bard *et al.* in the 1960s,[1–3] belongs to a special chemiluminescence (CL) triggered by voltage.[4] ECL contains electrochemical excitation and light radiation processes.[5] The electrochemical process provides the intermediates needed for CL reaction. The CL process is the interaction between these intermediates or between intermediates and other components in the system to produce an excited luminophore, and then the ECL signal can be observed as long as the emitter returns to its ground state.[6,7] Different emission mechanisms of ECL have been reported extensively from the beginning to the present, including annihilation ECL,[8–10] coreactant ECL,[11–13] thermoelectron induced ECL[14–16] and electrostatic ECL.[17,18] The earliest and relatively mature annihilation ECL is mainly suitable for organic phase systems, which is also the basis for the construction of various ECL light-emitting devices (ECLD).[19,20] Annihilating ECL can be observed from organic molecules and metal–organic complexes, such as rubrene,[21,22] porphyrin,[23–25] cyclometalated platinum(II) complexes[26] and iridium(III) complexes.[27,28] However, serious quenching, due to various impurities, results in the inability of annihilation ECL to be used in more popular aqueous media. After a lot of exploration, the emergence of the coreactant mechanism perfectly compensates for the above shortcomings, which enables ECL technology to be widely employed in aqueous detection systems. These luminophores capable of a coreactant mechanism are mainly water-soluble organic molecules, nanomaterials and some heterocyclic compounds with aggregation-induced emission (AIE) effects, such as Lucigeni,[29] luminol,[30] $Ru(bpy)_3^{2+}$,[31] graphene quantum dots,[32] Sulfur quantum dots,[33] CdZnSe nanocrystals,[34] and tetraphenylsiloles.[2,35] Controllability of time and space is a significant advantage of ECL over CL, and neglectable background interference can also be achieved, compared to photoluminescence (PL), due to the absence of additional excitation sources.[36]

The signal readout of ECL includes intensity mode (converting optical signals into electrical signals *via* photomultiplier tubes) and spectral mode (collecting optical signals directly using spectrometer).[37] The change of ECL intensity can monitor the fluctuation of the concentration of the analyte under the intensity mode, which is the premise of sensor construction,[38] and the spectral model is more conducive to exploring the internal information of the luminophore to achieve the goal of optimizing the ECL efficiency.[39] ECL has formed a set of perfect theory and application system after more than 60 years of development and improvement.[40] The introduction of various types of luminophores has enabled ECL technology to be employed in organic, aqueous and living organisms. The application of ECL has expanded from the original sensor to imaging, devices and characterization.[41–50] In this review, we focus on classifying different varieties of luminophores into the following three categories, including single molecules, nanostructured materials and heterocyclic compounds with AIE effects. Moreover, the applications of ECL in many fields (sensor, imaging, device

[a] *Tianjin Key Laboratory of Molecular Optoelectronic, Department of Chemistry, School of Science, Tianjin University, Tianjin, 300072, P. R. China. E-mail: luxq@tju.edu.cn*
[b] *Key Laboratory of Bioelectrochemistry & Environmental Analysis of Gansu Province, College of Chemistry & Chemical Engineering, Northwest Normal University, Lanzhou, 730070, P. R. China. E-mail: luxq@nwnu.edu.cn*
† Z. Z., P. D. and G. P. contributed equally to this work.

and characterization) have also been systematically summarized in the current review.

2. Classification of ECL Luminophores

2.1 Single molecule luminophore

Such luminophores are generally hydrophilic or lipophilic organic compounds or metal complexes. They dissolve well in aqueous or oil phase, and can exist in a system as a single molecule. Single molecule luminophores generally have a relatively high luminous efficiency. Qi's group has reported that 1,3,5-tris(decyl-10-)benzene has strong ECL properties in a mixed solution of acetonitrile and acetone.[51] Its three different derivatives, T1, T2, and T3, are shown in Fig. 1. By electrochemical and ECL testing of the three derivatives, T1 and T2 have three reversible single electron transfer processes throughout the redox process, while T3 has six reversible single electron transfer processes. All three derivatives can produce a strong and stable blue ECL phenomenon through the quenching mechanism. And the ECL spectra of these three derivatives are consistent with their respective fluorescence spectra. The above results show that T1–T3 have great application prospects in the ECL field in the future due to their distinctive electrochemical and optical properties.

Xu *et al.* found that containing the dipyrido[3,2-*a*:2′,3′-*c*]phenazine (dppz) ligand, $[Ru(bpy)_2dppz]^{2+}$ exhibits a remarkable ECL enhancement upon intercalation into the nucleic acid structure.[52] Based on the unique structure, $[Ru(bpy)_2dppz]^{2+}$ can also be used to develop a label-free, sensitive, and selective ECL platform for ATP detection. Zhu's team also reported that a graphene oxide (GO) drop on the surface of the glassy carbon electrode (GCE), $Ru(bpy)_3^{2+}$ generates a strong anode ECL signal, indicating that GO itself can act as a co-reactant of $Ru(bpy)_3^{2+}$.[31] The system can be used to construct an ECL biosensor to immobilize a thiol-terminated adenosine triphosphate (ATP) aptamer on a GO membrane by DNA hybridization. When the gold nanoparticle/graphene oxide (AuNPs/GO) nanocomposite was modified on the aptamer by a S–Au bond to form a sandwich structure, ECL resonance energy transfer (ECL-RET) occured between the $Ru(bpy)_3^{2+}$ and AuNPs/GO nanocomposites, resulting in a significant decrease in ECL intensity. If the ECL sensor is immersed in ATP solution for a while, due to the specific recognition between the aptamer and ATP, the AuNPs/GO nanocomposite will detach from the electrode surface, eventually leading to an increase in the intensity of ECL. The ECL aptamer sensor based on the above principle can be used for highly sensitive and selective detection of ATP. The linear range of detection of ATP is 0.02–2 pM, and the minimum detection limit is 6.7 fM (S/N = 3). The mechanism of detection is shown in Fig. 2.

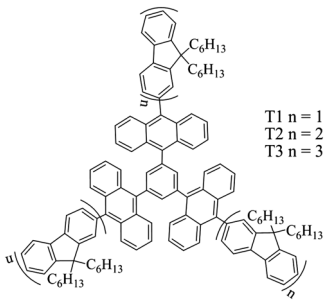

Fig. 1 Structures of T1 to T3.[51] Reprinted with permission from ref. 51. Copyright 2016 American Chemical Society.

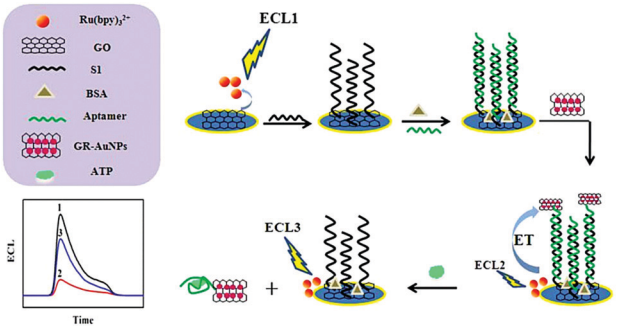

Fig. 2 A schematic representation of the modification of the GCE and the detection of ATP.[31] Reprinted with permission from ref. 31. Copyright 2016 American Chemical Society.

Many metal complexes and clusters can produce ECL.[53–55] However, due to the coupling of the spin orbits, the spin of the transition metal compound allows the excited state to be rapidly deactivated, and the luminescence is mainly returned from the lowest energy excited state to the ground state.[28] In most cases, the lifetimes of these excited species are very short, and the light emission mainly comes from the phosphorescence generated by the spin-forbidden excited state. ECL of metal complexes such as Ru, Os, Cr, Cd, Pd, Pt, Re, Ir, Mo, Tb, Eu, Cu, and Al has been studied. For some metals, such as Ru, Os, and Re, considering the effect of different ligands on the ECL properties of the complexes, researchers have studied the properties of a series of different ligands corresponding to them. The structure of the ligand is appropriately modified, and the modified complex may be immobilized on the electrode or bound to different analytes.

2.2 Nanomaterial luminophore

As a new kind of ECL luminophore, nanomaterials have many advantages, such as hydrophilic and hydrophobic control, convenient synthesis and controllable ECL radiation wavelength. Due to its unique photoelectric properties, the applications of nanomaterials in the field of ECL have attracted widespread attention. According to the different morphologies, the luminaries of nanomaterials are mainly divided into quantum dots, nanoclusters and nanosheets.

2.2.1 Quantum dots (QDs). As early as 1983, Brus *et al.* discovered colloidal semiconductor nanocrystals or quantum dots (QDs).[56,57] This discovery ushered in a new era in nanoscience and nanotechnology. Quantum dots are monodisperse clusters of crystals whose physical size (usually within a few nanometers) is smaller than the Bohr radius of the bulk exciton, that is the distance between the electron–hole (e–h) pair.[58] In the past few decades, a large number of experimental and theoretical research studies have been reported on the unique chemical and physical properties of quantum dots.[38,59]

In 2002, Ding's research group first reported the ECL phenomenon of silicon quantum dots (Si QDs).[60] They observed by differential pulse voltammetry (DPV) in *N*,*N*′-dimethyl formamide and acetonitrile that discrete quantities of electrons could be reversibly injected into spatially stable silicon nanocrystals (NC) (diameters 2–4 nm). The electrochemical band gap between electron and hole transfer (related to the highest and lowest occupied molecular orbitals) increases with the decrease in the size of the nanocrystals. The initial potential of electron injection is approximately equivalent to the expected coulomb blockade or quantized double charge energy. Electron transfer reactions between positively or negatively charged nanocrystals (or between charged nanocrystals and co-reagents) result in electron–hole annihilation, which eventually produces visible ECL signals. The maximum peak of the ECL spectrum of Si QDs was located at 640 nm, exhibiting a significant red shift compared with its fluorescence radiation peak (420 nm). These results indicate that Si QDs possess very stable photoelectric characteristics and can be used in the ECL system as a new luminant.

According to Fig. 3A, the band gap on the surface of quantum dots is smaller than that inside. It is found that fluorescence radiation is the light signal radiated by the excited electrons inside the quantum dot, while ECL is the light signal radiated by the excited electrons on the surface. Therefore, the ECL spectrum will show red-shift relative to its PL spectrum in general. But when the surface of a quantum dot is smooth enough, the electrons can overlap completely in the ECL and PL spectra. In addition, the surface of quantum dots can also be doped to regulate the ECL spectrum of quantum dots directionally.[61]

They proposed a simple *in situ* activation method by fixing a CdS QD film on a glassy-carbon electrode (CdS QDs/GCE) containing H_2O_2 and citric acid activation solution, which increased the ECL strength of CdS QDs by about 58 times in the presence of co-reactive agent H_2O_2.[62] In the activation process, CdS QDs are oxidized by H_2O_2 to smaller CdS QDs, resulting in more surface vacancies (as shown in Fig. 4). Citric acid plays an important role in the processes of stabilizing QDs. They studied the enhancement mechanism of ECL in detail, and proposed that the coordination between H_2O_2 and excess Cd^{2+} ions (S vacancies) on the CdS QDs surface was the main factor for stable electrogenic radicals, thus

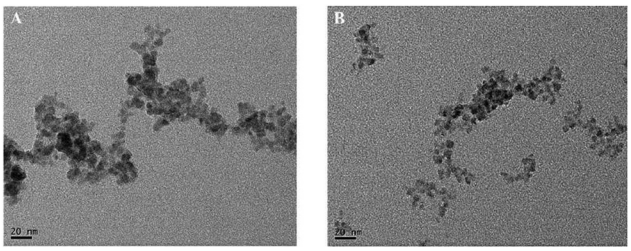

Fig. 4 Transmission electron microscopy (TEM) of the original CdS QDs (A) and the activated CdS QDs (B).[62] Reprinted with permission from ref. 62. Copyright 2014 American Chemical Society.

enhancing the ECL signal. Since S(II) can bind to excessive Cd^{2+} ions on the surface of CdS QDs, ECL signals of activated CdS QDs/GCE can be quenched in Na_2S solution. On this basis, they used activated CdS QDs/GCE as an ECL probe to detect Na_2S, and the results showed that this probe had good performance and strong anti-interference ability, with the linear detection range from 5 to 20 μm. In addition, this ECL probe has also been successfully applied to the detection of hydrogen sulfide (H_2S) in biological systems, and its detection mechanism is shown in Fig. 5.

In addition, common quantum dots include CdSe QDs,[63] CdSe@ZnS QDs,[64] CdTe QDs,[65] C QDs,[66–68] MoS_2 QDs[69] and polymer quantum dots.[70–73] These works provide extensive scientific basis for the research of ECL characteristics of quantum dots.

2.2.2 Metal clusters (NCS). The optical and electrochemical properties of most semiconductor quantum dots cannot meet the requirements due to the surface state induced effect. In addition, the low electrochemical luminescence efficiency also severely limits the practical application of quantum dots. However, metal nanocrystals such as gold nanocrystals become another new type of ECL laminator because of their stable optical and electrochemical properties, monodisperse size, low and well-defined bandgap, and high atomic accuracy.[74,75] Wang's research group has reported a gold nanocluster (AuNCs) wrapped with lipoic acids, which has strong ECL signal in aqueous solution.[76] They constructed a new strategy to significantly strengthen the ECL signal of AuNCs by covalently attaching the co-reactive agent

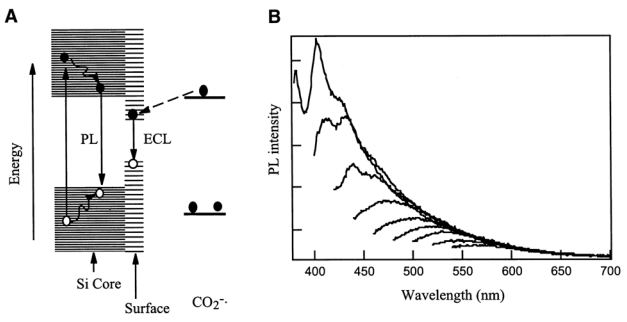

Fig. 3 (A) Schematic mechanisms for ECL and PL of Si clusters. (B) PL spectra at different excitation energies recorded with the same solution as in A.[60] Reprinted with permission from ref. 60. Copyright 2002 The American Association for the Advancement of Science.

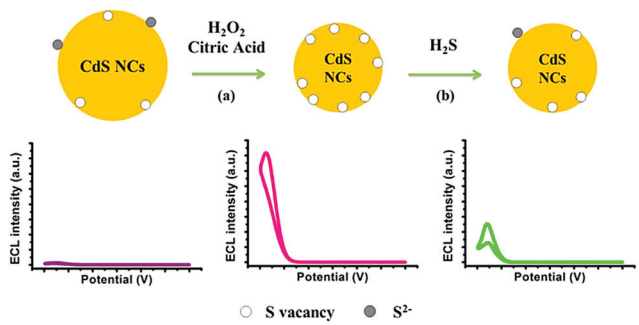

Fig. 5 (a) Schematic representation of activation of CdS QDs by H_2O_2 and citric acid (b) its application in H_2S detection based on the quenching effect of ECL emissions caused by adsorption of H_2S on the surface S vacancies.[62] Reprinted with permission from ref. 62. Copyright 2014 American Chemical Society.

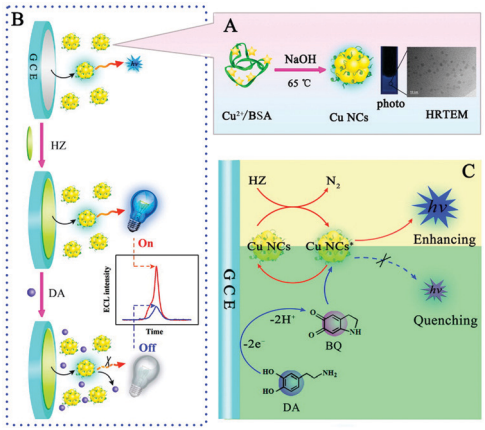

Fig. 6 (A) The preparation process of Cu NCs and the photo and typical HRTEM image of the as-prepared Cu NCs; (B) the sensing platform for DA detection based on the Cu NCs/HZ ECL system; (C) proposed ECL enhancing mechanism of the Cu NCs/HZ system and ECL quenching mechanism by DA toward the Cu NCs/HZ system.[77] Reprinted with permission from ref. 77. Copyright 2016 American Chemical Society.

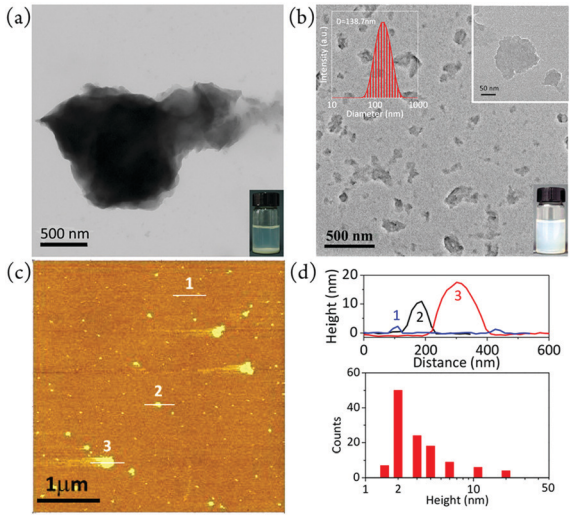

Fig. 7 TEM images of (a) pristine bulk CN and (b) m-CNNS. Inset in (a) shows a photo of bulk CN dispersion with some suspended solid, and insets in (b) show a photo and the DLS size distribution of the mCNNS dispersion. (c) AFM image of m-CNNS. (d) Height profiles of the points marked in (c) and height statistics of m-CNNS (N = 118) using the AFM data in (c).[79] Reprinted with permission from ref. 79. Copyright 2017 American Chemical Society.

N,*N*-diethylethylenediamine (DEDA) to AuNCs stabilized by octanoic acid. The material is designed and synthesized to reduce the complexity of proton transfer between free radical intermediates involved in conventional ECL reaction pathways. By eliminating additional and energy-intensive co-reactants, the cluster reaction is more practical. The enhanced ECL efficiency is due to multiple energy states of each Au cluster and multiple DEDA ligands in a single layer. Obviously, this strategy of attaching co-reactants to AuNCs is also applicable to other nanomaterials.

The cathodic ECL behavior of Cu NCs in aqueous solution was first reported by Yuan's research group.[77] Cu NCs can produce a strong and stable ECL signal after hydrazine (HZ) is added. Based on this novel agent, they have constructed a sensitive "signal switch" type dopamine (DA) sensing platform with a detection limit of 3.5×10^{-13} M. The preparation process and ECL detection mechanism of Cu NCs are shown in Fig. 6. The proposed Cu NCs provide a powerful basis for the preparation of cheap and non-toxic luminous agents.

2.2.3 Other nanomaterials. Graphite phase carbon nitride (CN), as a new type of nitrogen-rich two-dimensional carbon material, has been widely used in the fields of photo/electrocatalysis and biosensors. The interface modification of CN is very significant for its practical application, especially for the regulation of its ECL characteristics. Zhang *et al.* have performed a large number of systematic studies on the application of graphite phase carbon nitride (CN) in the field of electrochemiluminescence.[78,79] They used a simple mechanical grinding method to destroy the pi-pi stacking between layers of CN, so as to cut the large CN into a smaller size (as shown in Fig. 7a and b). The prepared CN nanocrystals (CNNS) not only retain the photoelectric properties of the original CN, but also overcome the shortcomings of CN on the material surface, providing a strong basis for its further application in the field of biosensors. Finally, they further covalently linked m-CNNS with DNA probes, resulting in a targeted DNA electrochemical luminescence biosensor with higher sensitivity than the unmodified CNNS sensor (direct physical adsorption of DNA probes). The detection process and mechanism are shown in Fig. 8. This kind of non-covalent stripping and interface modification will greatly expand the application scope of CN in biosensors and other application fields.

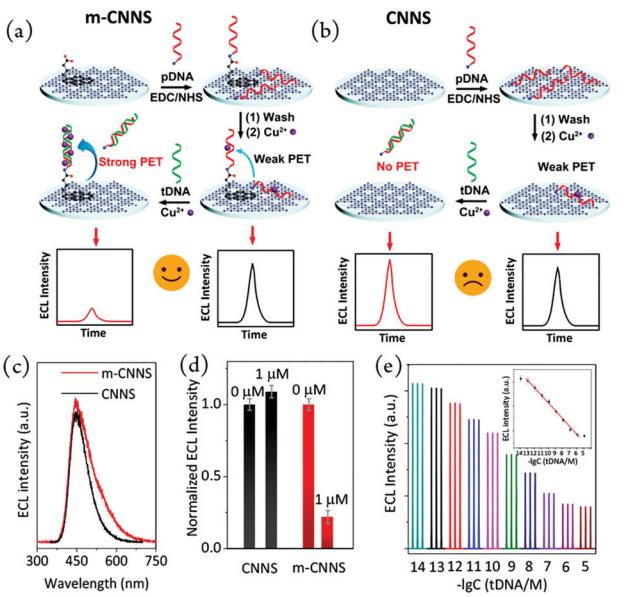

Fig. 8 Preparation of an ECL biosensor on a glassy carbon electrode using m-CNNS (a) and conventional CNNS (b). ECL emission spectra of mCNNS and CNNS (c). ECL intensity of m-CNNS- and CNNS-based biosensors upon addition of 0 and 1 μM tDNA (d). ECL response of mCNNS upon addition of 10^{-14}–10^{-5} M tDNA (e). Inset: Scatter plot and linear fitting of ECL intensity *vs.* concentration.[79] Reprinted with permission from ref. 79. Copyright 2017 American Chemical Society.

Meanwhile, this method is also suitable for the interface control of other two-dimensional materials.

In addition, other common nanomaterials include $CsPbBr_3$ nanocrystals,[80] wurtzite ZnSe,[81] nanoscale disks,[82] and nanotubes.[83] The development and utilization of these new ECL brighteners have established a solid foundation for the future development of ECL.

2.3 AIE luminophore

Aggregation-induced luminescence (AIE) is a photophysical phenomenon associated with the accumulation of luminescent agents, which was first proposed by the Tang team in 2001.[84–87] In the AIE process, the originally monodisperse illuminant radiates light due to aggregation.[88] This mechanism has been successfully applied in the fields of organic light emitting diodes (OLEDs),[89,90] biological probes,[91–93] chiral recognition,[94] photodynamic cancer therapy and polarization luminescence.[95–97] Cola's group proposed that platinum complex supramolecular nanomaterials can lead to a strong ECL emission,[53] as shown in Fig. 9. Prior to this, there has been no report on the co-reactant type ECL phenomenon of platinum complexes in the aqueous phase. The main reason is that the synthesis process of the luminescent agent is complicated, and it is difficult to find a co-reactant that matches the potential of the illuminant. For the first time, they successfully applied the mechanism of aggregation-induced luminescence to the field of ECL and defined it as aggregation-induced ECL (AIECL). In their work, they studied the photophysical properties of two square planar Pt(II) complexes in solution and the solid state, as well as their ECL and AIECL properties. The experimental results show that the self-assembly of luminophores in the synthesis process changes their HOMO and LUMO energies, which can generate excited luminophores through the ECL pathway. These platinum complexes have a higher luminous efficiency than the $Ru(bpy)_3^{2+}$ luminous efficiency.

Recently, Ju's group synthesized two AIE-active DA-type conjugated polymers P-1 and P-2 containing fluorene, carbazole, tetrastyrene and BODIPY moieties by Suzuki reaction (Fig. 10).[72] Energy transfer inside the molecule can be achieved by using tetrastyrene as a bridge. This mechanism contributes to the enhancement of solid-state ECL signals. This work explores a new method to develop AIE-active ECL luminescent agents with low potential and strong ECL singnal by changing the D–A electronic structure. The discovery of this new type of AIE-active ECL luminescent agent could produce a new generation of ECL luminescent agents, which has great guide meaning and application value.

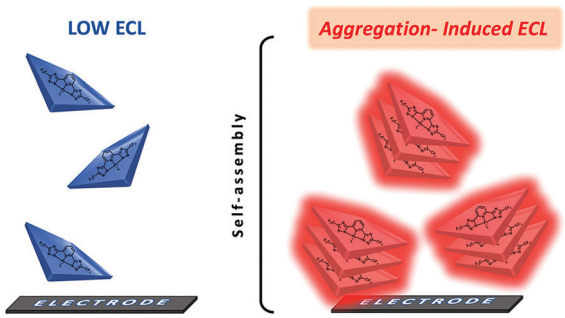

Fig. 9 Aggregation-induced electrochemiluminescence of square-planar Pt(II) complexes.[53] Reprinted with permission from ref. 53. Copyright 2017 American Chemical Society.

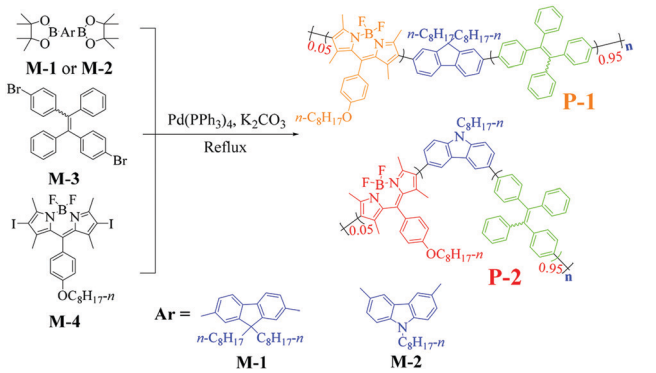

Fig. 10 Synthetic routes of P-1 and P-2.[72] Reprinted with permission from ref. 72. Copyright 2018 American Chemical Society.

3. Applications of ECL

3.1 ECL sensors

As a highly sensitive analytical technique, lots of ECL-based sensors have been developed. Take the $Ru(bpy)_3^{2+}$/TPrA system as an example, in which $Ru(bpy)_3^{2+}$ is used as a luminophore and TPrA is used as a coreactant.[98–100] This system has many obvious advantages, such as simple operation, rapid analysis, high sensitivity and wide detection range, which is considered as one of the most successful luminophores with very broad applications. With annual sales of hundreds of millions of dollars, more than 150 ECL immunosensors are currently available for commercial testing. ECL sensors are mainly classified into the following categories depending on the object to be detected.

3.1.1 The detection of organic/inorganic/biological small molecules. The detection mechanism of such sensors is generally that the analyte can directly or indirectly interact with the luminophore or the coreactant, thereby enhancing or attenuating the ECL signal, and finally achieving linear detection of the analyte.[101,102] The signal output can be in a single or multiple ECL intensity mode or an ECL spectral output mode. For example, high-sensitivity *in situ* detection of molecules released by living cells is of great significance in pathophysiological studies. In response to the above problems, Yuan *et al.* prepared a new type of ECL luminophore, namely *N*-(aminobutyl)-*N*-(ethylisoluminol)-functionalized Ag nanoparticle modified three-dimensional (3D) polyaniline–phytic acid conducting hydrogel (ABEI–Ag@PAni–PA), which can be used to detect hydrogen peroxide (H_2O_2) released by living cells *in situ*.[103] The three-dimensional nanostructure ABEI–Ag@PAni–PA conductive hydrogel combines the advantages of conductive hydrogels and nanoparticle catalysts. PAni–PA conductive hydrogel has good biocompatibility, a porous structure and a three-dimensional structure continuity, which is beneficial to the cell adhesion and high load density of ABEI–Ag luminescent

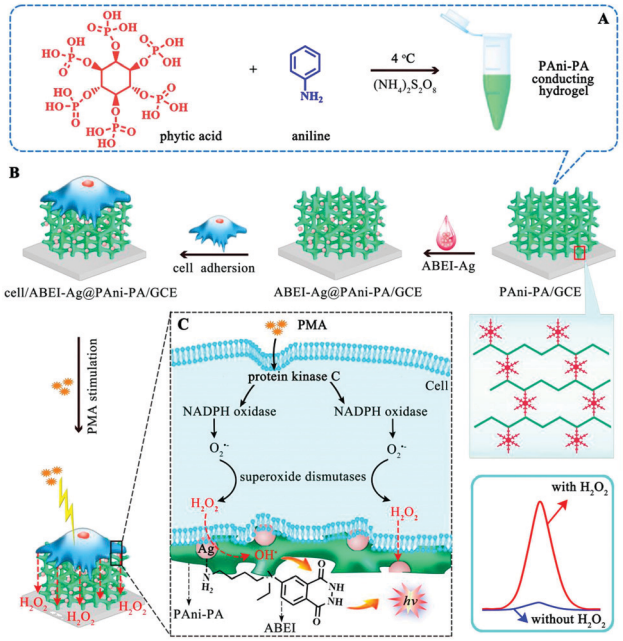

Fig. 11 Schematic illustration of (A) the fabrication procedure of the ABEI–Ag@PAni–PA conducting hydrogel, (B) the preparation of the ECL biosensor for cell assay, and (C) the H_2O_2 production path triggered by the PMA and ECL reaction mechanism.[103] Reprinted with permission from ref. 103. Copyright 2018 American Chemical Society.

materials. Compared with the traditional method for detecting H_2O_2, ABEI–Ag@PAni–PA conductive hydrogel can achieve cell adhesion, which enables sensitive *in situ* monitoring of H_2O_2 released by drugs under drug stimulation. The detection process is shown in Fig. 11.

The ECL spectrum can also be used for quantitative detection of analytes, which is similar to fluorescent sensors. Xu's group has proposed a single-electrode CL system for multiplex ECL analysis of hydrogen peroxide, glucose and uric acid simultaneously. With favorable simplicity and versatility, this single-electrode CL system is very promising for broad detection applications.[104] Zhang's group has reported a wavelength-resolved ECL biosensor and used it to simultaneously detect many biomarkers on a single working electrode interface.[105] A high-resolution ECL spectral detection system (shown on the left in Fig. 12) was established by combining

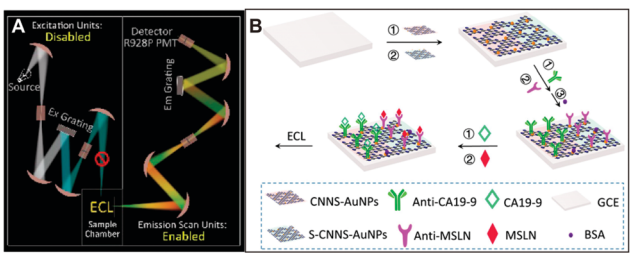

Fig. 12 Scheme of a tabletop spectrofluorometer-potentiostat system for high-resolution ECL spectrum collection, and diagram of the light path (left); general assembly procedure for the wavelength-resolved ECL biosensor for the simultaneous detection of multiple biomarkers (right).[105] Adapted with permission from ref. 105. Copyright 2018 American Chemical Society.

a potentiostat and a fluorescence spectrometer. The ECL biosensor has high accuracy and sensitivity in simultaneously detecting multiple PDAC biomarkers in spiked serum (as shown on the right in Fig. 12). This technology opens up a new way for the application of ECL in the field of sensing.

3.1.2 The detection of antigen/antibody. Due to the strong interaction between antigen and antibody, the ECL antigen/antibody detection method has broad application prospects in clinical sample analysis. This kind of sensor plays an important role in the diagnosis of diseases such as cancer by measuring certain tumor-associated markers. The mechanism of the ECL antigen/antibody detection method generally utilizes the specific binding effect between the antigen and the antibody, and fixes or detaches the luminescent agent to the surface of the electrode, thereby causing a regular change of the ECL signal and achieving the linear detection purpose of the object to be tested. For example, prostate specific antigen (PSA) is the best serum marker for current diagnosis and early localization of prostate cancer. Wei's group constructed a novel unlabeled PSA immunosensor based on Ag-NPs-doped Pb(II)-β-CD(Ag@Pb(II)-β-CD).[106] Subsequently, they synthesized amidated graphene (NH_2-Gr) and gold nanoparticle (NP) functionalized cerium oxide (CeO_2) nanoparticles (NH_2-Gr/Au@CeO_2). The prepared NH_2-Gr/Au@CeO_2 has strong ECL activity and can be effectively quenched by bismuth sulfide (Bi_2S_3). Based on this principle, they constructed a sandwich ECL immunosensor for PSA detection. NH_2-Gr acts as a supporting matrix for CeO_2 nanoparticles because of its good conductivity and large specific surface area Anti-PSA 1 (Ab1) and CeO_2 are linked by Au NPs, and Au NPs also have an effect of enhancing conductivity. Using NH_2-Gr/Au@CeO_2 as the ECL response layer, the Bi_2S_3 labeled secondary antibody (Ab_2) was functionalized with Ag-NP, and the ECL signal of the luminescent agent was significantly quenched by the immunoreaction between the antigen and antibody. This switch-type immunosensor has the advantages of wide linear response range and low detection limit.

In addition to the conventional single-channel detection technology, Zou's group recently constructed a multi-channel ECL immunosensor to simultaneously detect multiple analytes in a single system.[107] They proposed a spectrally resolved three-color ECL composite immunoassay (MIA), and then explored the monochromatic ECL from dual-stabilizers-capped CdTe and CdSe NCs, and found the inherent lower background of ECL than PL. Finally, carcinoembryonic antigen (CEA), prostate specific antigen (PSA) and alpha-fetoprotein (AFP) were used as model analytes to form three antigen-NCs on the surface of a glassy carbon electrode (GCE) by the immunological reaction with CdSe(550), CdTe(650), and CdTe(776) NCs as tags, respectively. Different antigen-NCS will produce an ECL response to different analytes, and the maximum ECL intensity of each tag determines the corresponding antigen. The advantage of this technique is that no optical filters or signal splitters are required. This ECL-MIA sensor has extremely low cross-reactivity, high color-selectivity and excellent sensitivity with detection limits of 1, 10 and 0.01 pg ml^{-1} for CEA, PSA and AFP, respectively. The detection mechanism of this sensor is shown in Fig. 13.

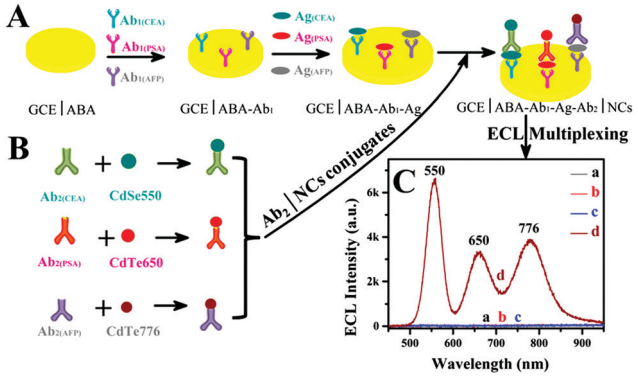

Fig. 13 Schematic illustration of spectral ECL-MIA.[107] Reprinted with permission from ref. 107. Copyright 2018 American Chemical Society.

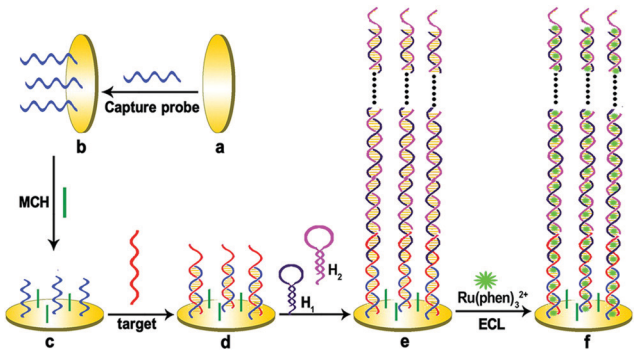

Fig. 14 A schematic representation of the preparation of the hybridization chain reaction-based ECL DNA sensor.[108] Reprinted with permission from ref. 108. Copyright 2012 American Chemical Society.

3.1.3 The detection of DNA. The ultra-micro detection of DNA is of great significance in the fields of medical diagnosis, environmental investigation, gene expression analysis, drug research, homeland security and forensic analysis. ECL is a highly sensitive and specific detection technology that can detect DNA. The ECL-DNA assay includes both unlabeled and labeled detection types. Compared with the mark ECL test, the mark-free ECL test has the advantages of time saving, low cost, simple operation and good reproducibility. In addition, in order to increase the sensitivity of DNA detection, a variety of signal amplification techniques are commonly employed. Signal amplification is mainly due to the ability of double-stranded DNA to adsorb large amounts of ECL luminescent agents (Fig. 14). Yuan's group used the *in situ* hybridization chain reaction signal amplification technique to construct a highly sensitive millimolar DNA unlabeled ECL detection method.[108] This method has better sensitivity than other commonly used amplified DNA detection protocols.

3.2 ECL imaging

ECL is a technology that generates optical signals by electrical excitation. This process can be precisely controlled by potential and without interference from background light signals. Therefore, ECL has a bright and broad application prospect in the field of imaging. The imaging objects mainly include fingerprints, cells, and nanomaterials.

3.2.1 Fingerprint imaging. Fingerprints are impressions of the friction ridge pattern left by human fingertips after touching a surface. The whole area can be divided into hydrophobic area and hydrophilic area. They can serve as an indispensable tool in forensic investigations and personal identification, as well as for many other purposes in our daily life, such as safety inspection, access control, and individual credentials. Depending on the hydrophilicity of the ECL luminophores, we can use ECL technology to selectively image pro-/hydrophobic regions, or simultaneously image both regions to enhance the authenticity and reliability of the fingerprint. The Su group has developed two modes to identify fingerprints (negative and positive imaging).[66,109] Based on the different polarity of illuminants, the ECL fingerprint pattern is selectively presented on the surface of the electrode, as shown in Fig. 15.

3.2.2 Cell imaging. Single-cell microscopy has become the basic diagnostic tool for modern medicine and biology. At present, the ultrasensitive and quantitative detection of single cell membrane proteins mainly depends on the imaging of fluorescent probes. The fluorescent probes are immobilized on the cell membrane surface by *in situ* hybridization and immune reaction, which will produce a single cell fluorescence imaging.[110] ECL is a new imaging technology that combines the advantages of electrochemical sensitivity and high spatial resolution.[111] Since the ECL is an electrical excitation process, no extra light source is required, which greatly reduces the interference of the background signal. In addition, ECL cell imaging offers other advantages such as high sensitivity, good time and spatial resolution, high stability, versatility and low manufacturing costs.[112]

Sojic *et al.* recently reported an ECL-based surface area imaging technique that enables imaging of single-cell plasma membranes.[113] The principle is shown in Fig. 16. Through PL, ECL and AFM images of mammalian CHO cells, they demonstrated that ECL emission is limited to the adjacent area on the

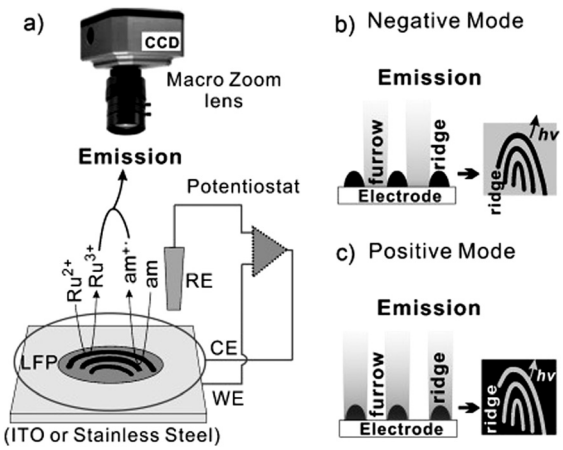

Fig. 15 (a) The ECL imaging system: Ru^{2+} and am represent the ECL generating luminophore and the amine co reactant, respectively. (b and c) The imaging strategy for visualizing LPFs in the negative (b) and positive (c) mode.[109] Reprinted with permission from ref. 109. Copyright 2012 Wiley-VCH Verlag GmbH & Co. KGaA, Weinheim.

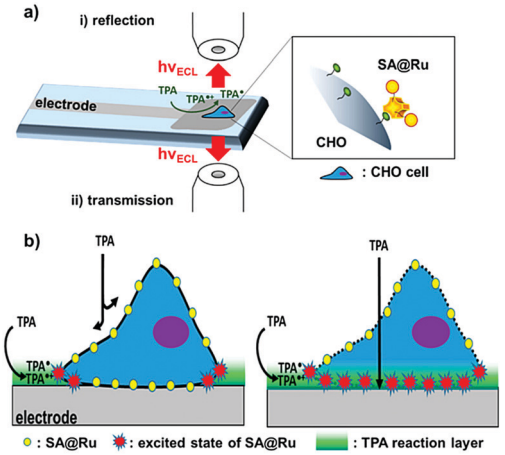

Fig. 16 Surface-confined ECL microscopy of labeled cells (a) in reflection configuration with the GC electrode or (b) in transmission configuration through the transparent CNT inkjet-printed electrodes.[113] Reprinted with permission from ref. 113. Copyright 2018, American Chemical Society.

electrode surface, and only the basement membrane of the cell can emit light, which is related to wide field fluorescence imaging. This is the opposite of wide field fluorescence imaging. The ECL microscope overcomes the challenges that classical fluorescence microscopy cannot solve without any light illumination and specific settings. In addition, since the generated radical lifetime is short and the diffusion distance is limited, the ECL emission region has a thickness of 500 nm. This ECL imaging is a dynamic technique that can be used not only for specific marker imaging of membranes, but also for reflecting the dynamic transport properties of cell membranes.

3.2.3 Nanomaterial imaging. As a probe technology, ECL provides a new perspective for the morphology and catalytic performance of nanomaterials. ECL microscopy also enables rapid and sensitive detection of the shape of individual nanoparticles as well as the electrochemical activity at the nanoscale.[114] The Willets team has reported the imaging of ECL signals from individual gold nanowires on tin-doped indium oxide electrodes.[115] The ECL imaging technology enables imaging of all gold nanowires in a given area without the need for an external light source or probe scanning. They also found that if the surface of the electrode is covered with a conductive polymer film, the imaging sharpness of the gold nanowire is greatly improved (as shown in Fig. 17).

In addition, nanomaterials of other shapes and sizes can also be imaged by ECL techniques, such as single gold nanoparticles,[116] polymer quantum dots,[58] and enzyme catalytic sites on nanomaterials.[65]

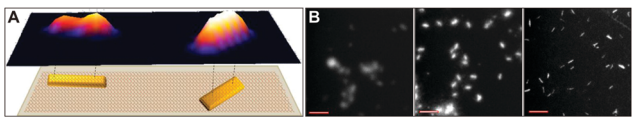

Fig. 17 ECL images of gold nanowires coated with $Ru(bpy)_3^{2+}$-doped PEDOT:PSS–PVA of different thicknesses.[115] Adapted with permission from ref. 115. Copyright 2015 American Chemical Society.

3.3 ECL devices

ECL devices (ECLDs) are different from conventional light-emitting diodes (LEDs) and organic light-emitting diodes (OLEDs).[10,26,117] The construction of ECLD does not require a hole transport layer (HTL) and an electron transport layer (ETL). It only requires two electrodes and a light-emitting layer, which does not need to consider the energy level relationship between layers.[20] This advantage greatly reduces the production cost of the device. As early as the beginning of ECL development, research on ECLD was reported. The luminescence mechanism can be divided into the following four processes: oxidation/reduction of luminescent agents on the surface of the electrodes (charge injection), diffusion of the intermediates (charge transfer), charge transfer reaction between the intermediates (excitation process), and excited state returns to the ground state (radiation of light).[118] The early ECLD was mainly constructed based on ionic liquids, and the luminescent agent was mainly tripyridinium ($Ru(bpy)_3^{2+}$).[19,119,120] The mechanism is to generate luminescence by collision between free radical anions and cations (as shown in Fig. 18).[118,121,122] However, ionic liquid type ECLD is difficult to be mass-produced, and the stability of ionic liquids is difficult to ensure.[8,119] Therefore, the first generation of ECLD based ionic liquids can only be used to study its luminescence mechanism.

Until 2014, ionic gels were widely reported and applied. Frisbie and others successfully constructed a series of solid ECLDs using ionic gels as illuminant carriers (as shown in Fig. 19).[123] Due to the nature of the ionic gel itself, it is stable in the environment, and the morphology is easily controlled. Therefore, the second generation of ECLD based on ionic gel has developed by leaps and bounds, and such devices have good luminous intensity and stability.[124] These provide an important basis for the commercial application of ECLD.[9,121]

In addition to improvements in luminescent agents and electrolytes, there are some studies on the improvement of working electrodes. For example, Barbara[30] proposed a gold-column array electrode (Fig. 20A), the Chen *et al.*[125] research team set up a needle tip nanoelectrode (Fig. 20B), and Parkinson[126] developed a cross-array electrode (Fig. 20C). These methods all improve the luminescence properties and stability of ECLD.

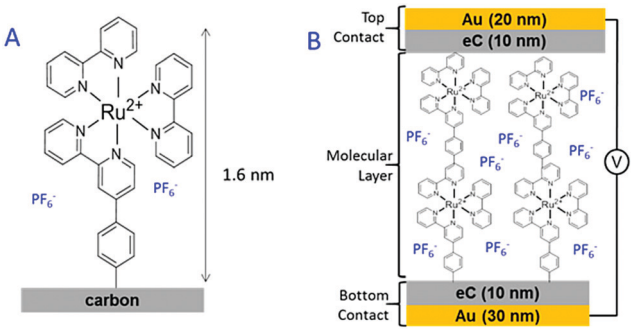

Fig. 18 (A) Structure of the $Ru(bpy)_3^{2+}$ molecular layer deposited on a carbon substrate. (B) A schematic illustration of the $Cr_4/Au_{30}/eC_{10}/Ru(bpy)_3P/eC_{10}/Au_{20}$ molecular junction.[119] Reprinted with permission from ref. 119. Copyright 2017 American Chemical Society.

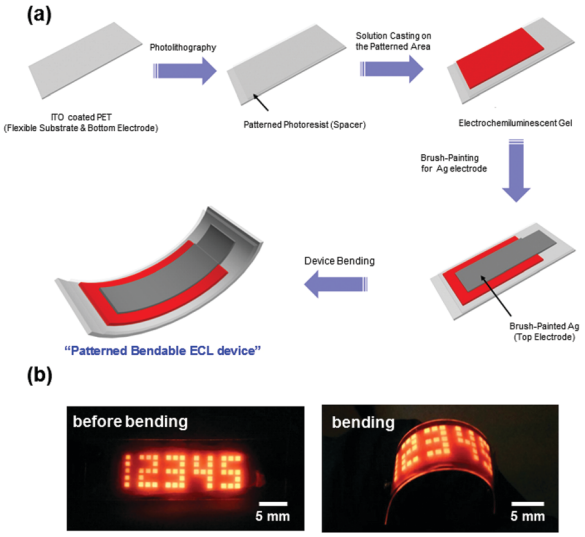

Fig. 19 (a) A schematic of the fabrication process for bendable ECL devices with patterned ECL gels on plastic. (b) Photographs of the ON states for fabricated ECL devices before bending (left image) and after bending (right image), where the applied voltage and frequency were VPP = 3.6 V (−1.8 to +1.8 V) and 60 Hz, respectively. The Arabic numerals are composed of 1 mm × 1 mm squares.[123] Reprinted with permission from ref. 123. Copyright 2014 American Chemical Society.

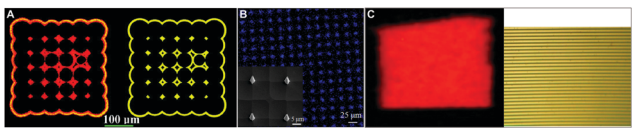

Fig. 20 The working electrode of different types of electroluminescent devices.[30,125,126] Adapted with permission from ref. 30, 125 and 126. Copyright 2011, 2017, and 2013 American Chemical Society.

3.4 ECL characterization technique

ECL reflects the photoelectric properties of the material, which offers an effective method to characterize the materials. Actually, the charge transfer pathway in the materials can be readily obtained *via* applying an appropriate voltage. Thus, it provides a fresh perspective to study the optical and electrochemical properties of materials by utilizing ECL. Xu *et al.* used ECL microscopy to image the electrocatalysis of a novel bimetallic Janus Au–Pt nanoparticle.[127] This new ECL imaging technique clearly shows that the Janus particle structure exhibited a superior catalytic performance than that of the individual nanoparticles (Fig. 21). Bard's research group has also used ECL behavior to investigate the photoelectric properties of phenanthrene derivatives with different substituent groups.[128] The results of binding different substituent groups into aromatic compounds can affect the luminescence efficiency and the stability of radical ions, and will guide the design and synthesis of new phenanthrene compounds. Dai *et al.* found that changing the crystal structure of ZnSe to nanocrystalline would remarkably influence the ECL performance, whereas the variation of ECL spectra reflected the crystal transformation. Therefore, ECL behavior can be used to predict the crystal defects and changes.[81]

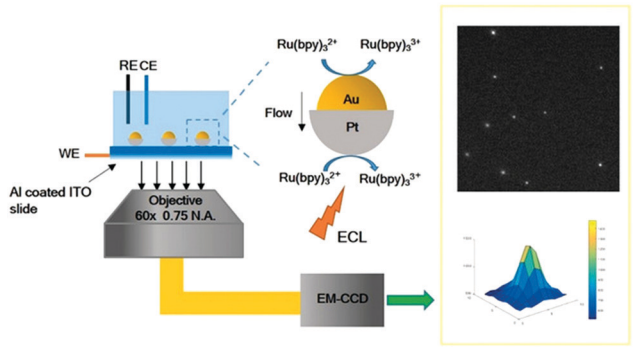

Fig. 21 Illustration of ECL imaging of electrocatalysis at Au–Pt JNPs.[127] Reprinted with permission from ref. 127. Copyright 2018 Wiley-VCH Verlag GmbH & Co. KGaA, Weinheim.

With further study, ECL characterization techniques will bring more and more material information.

4. Conclusions and perspectives

In this review, luminophores have been classified according to their respective characteristics; this will help us to understand the properties of ECL luminophores more systematically and deeply, and be conducive to the specific application of luminophores in the corresponding system. The reason why ECL technology can be widely used in humans, food, the environment, imaging, devices and other fields is due to the development of various luminophores with unique characteristics. In other words, the development of luminophores determines the velocity and prospect of ECL technology. In the future, the exploration of high efficiency and specific luminophores will be a hot topic in ECL research, which will make the application of ECL more extensive. Besides, ECL, as a technology that combines light and electricity perfectly, has many irreplaceable advantages; it has been used adroitly in many fields over the past 60 years. The extensive application of ECL in sensors, imaging, devices and characterization has fully demonstrated its irreplaceability. It is certain that more applications regarding ECL will be implemented in the future with the improvement of related technologies. Significantly, there are still many problems that need to be overcome in the process of supplementing ECL theory and expanding its applications.

Conflicts of interest

There are no conflicts to declare.

Acknowledgements

The authors would like to acknowledge the financial support given through The Natural Science Foundation of China (21575115 and 21705117), the Program of Gansu Provincial Higher Education Research Project (Grant No. 2017-D-01) and the Program for Chang Jiang Scholars and Innovative Research Team, Ministry of Education, China (Grant No. IRT-16R61).

Notes and references

1 R. T. Dufford, D. Nightingale and L. W. Gaddum, *J. Am. Chem. Soc.*, 1927, **49**, 1858–1864.
2 N. Harvey, *J. Phys. Chem. C*, 1929, **33**, 1456–1459.
3 K. S. V. Santhanam and A. J. Bard, *J. Am. Chem. Soc.*, 1965, **87**, 139–140.
4 R. E. Visco and E. A. Chandross, *J. Am. Chem. Soc.*, 1964, **86**, 5350–5351.
5 M. M. Richter, *Chem. Rev.*, 2004, **104**, 3003–3036.
6 K. Muzyka, *Biosens. Bioelectron.*, 2014, **54**, 393–407.
7 Z. Liu, W. Qi and G. Xu, *Chem. Soc. Rev.*, 2015, **44**, 3117–3142.
8 S. Tsuneyasu, K. Ichihara, K. Nakamura and N. Kobayashi, *Phys. Chem. Chem. Phys.*, 2016, **18**, 16317–16324.
9 T. Nobeshima, M. Nakakomi, K. Nakamura and N. Kobayashi, *Adv. Opt. Mater.*, 2013, **1**, 144–149.
10 H. Al-Kutubi, S. Voci, L. Rassaei, N. Sojic and K. Mathwig, *Chem. Sci.*, 2018, **9**, 8946–8950.
11 M. Hesari, S. M. Barbon, R. B. Mendes, V. N. Staroverov, Z. Ding and J. B. Gilroy, *J. Phys. Chem. C*, 2018, **122**, 1258–1266.
12 A. S. Danis, K. P. Potts, S. C. Perry and J. Mauzeroll, *Anal. Chem.*, 2018, **90**, 7377–7382.
13 Y. He, L. Yang, F. Zhang, B. Zhang and G. Zou, *J. Phys. Chem. Lett.*, 2018, **9**, 6089–6095.
14 S. K. T. Ala-Kleme, L. Va1re, P. Juhala and M. Helin, *Anal. Chem.*, 1999, **71**, 5538–5543.
15 A. J. Nozik, *Annu. Rev. Phys. Chem.*, 2001, **52**, 193–231.
16 F. Gaillard, Y. E. Sung and A. J. Bard, *J. Phys. Chem. B*, 1999, **103**, 667–674.
17 A. K. S. Kulmala, A. Kulmala, D. Papkovsky and K. Loikas, *Anal. Chem.*, 1998, **70**, 1112–1118.
18 K. F. J. Kankare, S. Kulmala and K. Haapakka, *Anal. Chim. Acta*, 1992, **256**, 17–28.
19 E. S. Ko, J. I. Lee, H. C. Lim, J. E. Park, S. H. Kong, J. I. Hong, M. S. Kang and I. S. Shin, *ACS Photonics*, 2018, **5**, 3723–3730.
20 J. I. Lee, D. Kang, S. H. Kong, H. Gim, I. S. Shin, J. Kim and M. S. Kang, *ACS Appl. Mater. Interfaces*, 2018, **10**, 41562–41569.
21 D. L. Maricle and A. Maurer, *J. Am. Chem. Soc.*, 1967, **89**, 188–189.
22 Y. Li, L. Xu, Y. He and B. Su, *Electrochem. Commun.*, 2013, **33**, 92–95.
23 E. K. Galvan-Miranda, H. M. Castro-Cruz, J. Arturo Arias-Orea, M. Iurlo, G. Valenti, M. Marcaccio and N. A. Macias-Ruvalcaba, *Phys. Chem. Chem. Phys.*, 2016, **18**, 15025–15038.
24 G. Pu, D. Zhang, X. Mao, Z. Zhang, H. Wang, X. Ning and X. Lu, *Anal. Chem.*, 2018, **90**, 5272–5279.
25 G. Pu, Z. Yang, Y. Wu, Z. Wang, Y. Deng, Y. Gao, Z. Zhang and X. Lu, *Anal. Chem.*, 2019, **91**, 2319–2328.
26 A. K. Chan, M. Ng, Y. C. Wong, M. Y. Chan, W. T. Wong and V. W. Yam, *J. Am. Chem. Soc.*, 2017, **139**, 10750–10761.
27 M. A. Haghighatbin, S. C. Lo, P. L. Burn and C. F. Hogan, *Chem. Sci.*, 2016, **7**, 6974–6980.
28 M. B. Herbert, V. M. Marx, R. L. Pederson and R. H. Grubbs, *Angew. Chem., Int. Ed.*, 2013, **52**, 310–314.
29 W. Gao, Z. Liu, L. Qi, J. Lai, S. A. Kitte and G. Xu, *Anal. Chem.*, 2016, **88**, 7654–7659.
30 S. Guo, O. Fabian, Y. Chang, J. Chen, W. Lackowski and P. Barbara, *J. Am. Chem. Soc.*, 2011, **133**, 11994–12000.
31 Y. P. Dong, Y. Zhou, J. Wang and J. J. Zhu, *Anal. Chem.*, 2016, **88**, 5469–5475.
32 X. L. Cai, B. Zheng, Y. Zhou, M. R. Younis, F.-B. Wang, W. M. Zhang, Y. G. Zhou and X. H. Xia, *Chem. Sci.*, 2018, **9**, 6080–6084.
33 L. Shen, H. Wang, S. Liu, Z. Bai, S. Zhang, X. Zhang and C. Zhang, *J. Am. Chem. Soc.*, 2018, **140**, 7878–7884.
34 X. Zhang, X. Tan, B. Zhang, W. Miao and G. Zou, *Anal. Chem.*, 2016, **88**, 6947–6953.
35 Z. Han, Z. Yang, H. Sun, Y. Xu, X. Ma, D. Shan, J. Chen, S. Huo, Z. Zhang, P. Du and X. Lu, *Angew. Chem., Int. Ed.*, 2019, **58**, 5915–5919.
36 W. Miao, *Chem. Rev.*, 2008, **108**, 2506–2553.
37 Y. N. Khonsari and S. Sun, *Chem. Commun.*, 2017, **53**, 9042–9054.
38 X. Chen, Y. Liu and Q. Ma, *J. Mater. Chem. C*, 2018, **6**, 942–959.
39 C. Ma, W. Wu, Y. Peng, M. X. Wang, G. Chen, Z. Chen and J. J. Zhu, *Anal. Chem.*, 2017, **90**, 1334–1339.
40 M. Hesari and Z. Ding, *J. Electrochem. Soc.*, 2015, **163**, H3116–H3131.
41 J. Zhang, S. Arbault, N. Sojic and D. Jiang, *Annu. Rev. Anal. Chem.*, 2019, **12**, 275–295.
42 L. Qi, Y. Xia, W. Qi, W. Gao, F. Wu and G. Xu, *Anal. Chem.*, 2016, **88**, 1123–1127.
43 Y. Zhao, J. Yu, G. Xu, N. Sojic and G. Loget, *J. Am. Chem. Soc.*, 2019, **141**, 13013–13016.
44 X. Wang, E. Cao, H. Zong and M. Sun, *Appl. Mater. Today*, 2018, **13**, 298–302.
45 W. Lin, E. Cao, L. Zhang, X. Xu, Y. Song, W. Liang and M. Sun, *Nanoscale*, 2018, **10**, 5482–5488.
46 E. Cao, X. Guo, L. Zhang, Y. Shi, W. Lin, X. Liu, Y. Fang, L. Zhou, Y. Sun and Y. Song, *Adv. Mater. Interfaces*, 2017, **4**, 1700869.
47 W. Lin, X. Ren, L. Cui, H. Zong and M. Sun, *Appl. Mater. Today*, 2018, **11**, 189–192.
48 J. Wang, X. Mu and M. Sun, *Appl. Mater. Today*, 2019, **15**, 305–314.
49 R. Li, Y. Zhang, X. Xu, Y. Zhou, M. Chen and M. Sun, *Nanophotonics*, 2018, **7**, 873–881.
50 X. Mia, Y. Wang, R. Li, M. Sun, Z. Zhang and H. Zheng, *Nanophotonics*, 2019, **8**, 487–493.
51 H. Qi, C. Zhang, Z. Huang, L. Wang, W. Wang and A. J. Bard, *J. Am. Chem. Soc.*, 2016, **138**, 1947–1954.
52 L. Hu, Z. Bian, H. Li, S. Han, Y. Yuan, L. Gao and G. Xu, *Anal. Chem.*, 2009, **81**, 9807–9811.
53 S. Carrara, A. Aliprandi, C. F. Hogan and L. D. Cola, *J. Am. Chem. Soc.*, 2017, **139**, 14605–14610.
54 Y. Zhou, S. Chen, X. Luo, Y. Chai and R. Yuan, *Anal. Chem.*, 2018, **90**, 10024–10030.
55 Q. Zhai, H. Xing, X. Zhang, J. Li and E. Wang, *Anal. Chem.*, 2017, **89**, 7788–7794.

56 L. E. Brus, *J. Chem. Phys.*, 1984, **80**, 4403–4409.
57 A. P. Alivisatos, *Science*, 1996, **271**, 933–937.
58 M. Bruchez, M. Moronne, P. Gin, S. Weiss and A. P. Alivisatos, *Science*, 1998, **281**, 2013–2015.
59 J. Yao, L. Li, P. Li and M. Yang, *Nanoscale*, 2017, **9**, 13364–13383.
60 Z. Ding, B. M. Quinn, S. K. Haram, L. E. Pell, B. A. Korgel and A. J. Bard, *Science*, 2002, **296**, 1293–1297.
61 S. K. Poznyak, D. V. Talapin, E. V. Shevchenko and H. Weller, *Nano Lett.*, 2004, **2**, 693–698.
62 Y. Y. Zhang, H. Zhou, P. Wu, H. R. Zhang, J. J. Xu and H. Y. Chen, *Anal. Chem.*, 2014, **86**, 8657–8664.
63 N. Myung, Z. Ding and A. J. Bard, *Nano Lett.*, 2002, **2**, 1315–1319.
64 N. Myung, Y. Bae and A. J. Bard, *Nano Lett.*, 2003, **3**, 1053–1055.
65 Y. Bae, N. Myung and A. J. Bard, *Nano Lett.*, 2004, **4**, 1153–1161.
66 Y. He, L. Xu, Y. Zhu, Q. Wei, M. Zhang and B. Su, *Angew. Chem., Int. Ed.*, 2014, **53**, 12609–12612.
67 M. Amjadi, J. L. Manzoori, T. Hallaj and T. Shahbazsaghir, *Microchim. Acta*, 2017, **184**, 1587–1593.
68 S. Carrara, F. Arcudi, M. Prato and L. De Cola, *Angew. Chem., Int. Ed.*, 2017, **56**, 4757–4761.
69 M. Zhao, A. Y. Chen, D. Huang, Y. Q. Chai, Y. Zhuo and R. Yuan, *Anal. Chem.*, 2017, **89**, 8335–8342.
70 X. M. Shi, L. P. Mei, Q. Wang, W. W. Zhao, J. J. Xu and H. Y. Chen, *Anal. Chem.*, 2018, **90**, 4277–4281.
71 J. E. Dick, C. Renault, B. K. Kim and A. J. Bard, *J. Am. Chem. Soc.*, 2014, **136**, 13546–13549.
72 Z. Wang, Y. Feng, N. Wang, Y. Cheng, Y. Quan and H. Ju, *J. Phys. Chem. Lett.*, 2018, **9**, 5296–5302.
73 R. Dai, F. Wu, H. Xu and Y. Chi, *ACS Appl. Mater. Interfaces*, 2015, **7**, 15160–15167.
74 H. Jiang and X. M. Wang, *Chin. J. Anal. Chem.*, 2017, **45**, 1776–1785.
75 S. Han, Z. Zhang, S. Li, L. Qi and G. Xu, *Sci. China: Chem.*, 2016, **59**, 794–801.
76 T. Wang, D. Wang, J. W. Padelford, J. Jiang and G. Wang, *J. Am. Chem. Soc.*, 2016, **138**, 6380–6383.
77 M. Zhao, A. Chen, D. Huang, Y. Zhuo, Y. Chai and R. Yuan, *Anal. Chem.*, 2016, **88**, 11527–11532.
78 L. Chen, X. Zeng, P. Si, Y. Chen, Y. Chi, D. H. Kim and G. Chen, *Anal. Chem.*, 2014, **86**, 4188–4195.
79 J. Ji, J. Wen, Y. Shen, Y. Lv, Y. Chen, S. Liu, H. Ma and Y. Zhang, *J. Am. Chem. Soc.*, 2017, **139**, 11698–11701.
80 Y. Huang, X. Long, D. Shen, G. Zou, B. Zhang and H. Wang, *Inorg. Chem.*, 2017, **56**, 10135–10138.
81 S. Liu, Q. Zhang, L. Zhang, L. Gu, G. Zou, J. Bao and Z. Dai, *J. Am. Chem. Soc.*, 2016, **138**, 1154–1157.
82 X. Zhao, W. Zhou and C. Lu, *Anal. Chem.*, 2017, **89**, 10078–10084.
83 R. Wang, H. Wu, R. Chen and Y. Chi, *Small*, 2019, 1901550.
84 J. Luo, Z. Xie, J. W. Y. Lam, L. Cheng, B. Z. Tang, H. Chen, C. Qiu, H. S. Kwok, X. Zhan, Y. Liu and D. Zhu, *Chem. Commun.*, 2001, 1740–1741.
85 J. Mei, Y. Hong, J. W. Lam, A. Qin, Y. Tang and B. Z. Tang, *Adv. Mater.*, 2014, **26**, 5429–5479.
86 Y. Hong, J. W. Lam and B. Z. Tang, *Chem. Commun.*, 2009, 4332–4353.
87 H. Shi, S. Wang, L. Fang and B. Z. Tang, *Tetrahedron Lett.*, 2016, **57**, 4428–4434.
88 J. Mei, N. L. Leung, R. T. Kwok, J. W. Lam and B. Z. Tang, *Chem. Rev.*, 2015, **115**, 11718–11940.
89 H. Uoyama, K. Goushi, K. Shizu, H. Nomura and C. Adachi, *Nature*, 2012, **492**, 234–238.
90 T. H. Han, Y. Lee, M. R. Choi, S. H. Woo, S. H. Bae, B. H. Hong, J.-H. Ahn and T. W. Lee, *Nat. Photonics*, 2012, **6**, 105–110.
91 D. G. Khandare, H. Joshi, M. Banerjee, M. S. Majik and A. Chatterjee, *Anal. Chem.*, 2015, **87**, 10871–10877.
92 N. B. Shustova, B. D. McCarthy and M. Dinca, *J. Am. Chem. Soc.*, 2011, **133**, 20126–20129.
93 D. W. Domaille, E. L. Que and C. J. Chang, *Nat. Chem. Biol.*, 2008, **4**, 168–175.
94 X. Zhang, J. Yin and J. Yoon, *Chem. Rev.*, 2014, **114**, 4918–4959.
95 X. Gu, J. Yao, G. Zhang, Y. Yan, C. Zhang, Q. Peng, Q. Liao, Y. Wu, Z. Xu, Y. Zhao, H. Fu and D. Zhang, *Adv. Funct. Mater.*, 2012, **22**, 4862–4872.
96 J. Liu, H. Su, L. Meng, Y. Zhao, C. Deng, J. C. Y. Ng, P. Lu, M. Faisal, J. W. Y. Lam, X. Huang, H. Wu, K. S. Wong and B. Z. Tang, *Chem. Sci.*, 2012, **3**, 2737.
97 C. Shi, Z. Guo, Y. Yan, S. Zhu, Y. Xie, Y. S. Zhao, W. Zhu and H. Tian, *ACS Appl. Mater. Interfaces*, 2012, **5**, 192–198.
98 L. Hu and G. Xu, *Chem. Soc. Rev.*, 2010, **39**, 3275–3304.
99 L. Zhou, J. Huang, B. Yu, Y. Liu and T. You, *ACS Appl. Mater. Interfaces*, 2015, **7**, 24438–24445.
100 Q. Wang, M. Chen, H. Zhang, W. Wen, X. Zhang and S. Wang, *Biosens. Bioelectron.*, 2016, **79**, 561–567.
101 M. Wang, Y. Sun, J. Guo, X. Yang and M. Yang, *Chin. J. Anal. Chem.*, 2018, **46**, 780–786.
102 G. Li, X. Yu, D. Liu, X. Liu, F. Li and H. Cui, *Anal. Chem.*, 2015, **87**, 10976–10981.
103 X. Jiang, H. Wang, R. Yuan and Y. Chai, *Anal. Chem.*, 2018, **90**, 8462–8469.
104 W. Gao, K. Muzyka, X. Ma, B. Lou and G. Xu, *Chem. Sci.*, 2018, **9**, 3911–3916.
105 Y. Lv, Z. Zhou, Y. Shen, Q. Zhou, J. Ji, S. Liu and Y. Zhang, *ACS Sens.*, 2018, **3**, 1362–1367.
106 H. Ma, X. Li, T. Yan, Y. Li, Y. Zhang, D. Wu, Q. Wei and B. Du, *Biosens. Bioelectron.*, 2016, **79**, 379–385.
107 J. Zhou, L. Nie, B. Zhang and G. Zou, *Anal. Chem.*, 2018, **90**, 12361–12365.
108 Y. Chen, J. Xu, J. Su, Y. Xiang, R. Yuan and Y. Chai, *Anal. Chem.*, 2012, **84**, 7750–7755.
109 L. Xu, Y. Li, S. Wu, X. Liu and B. Su, *Angew. Chem., Int. Ed.*, 2012, **51**, 8068–8072.
110 G. Valenti, S. Scarabino, B. Goudeau, A. Lesch, M. Jovic, E. Villani, M. Sentic, S. Rapino, S. Arbault, F. Paolucci and N. Sojic, *J. Am. Chem. Soc.*, 2017, **139**, 16830–16837.
111 G. Liu, C. Ma, B. K. Jin, Z. Chen and J. J. Zhu, *Anal. Chem.*, 2018, **90**, 4801–4806.

112 J. Zhou, G. Ma, Y. Chen, D. Fang, D. Jiang and H. Y. Chen, *Anal. Chem.*, 2015, **87**, 8138–8143.
113 S. Voci, B. Goudeau, G. Valenti, A. Lesch, M. Jovic, S. Rapino, F. Paolucci, S. Arbault and N. Sojic, *J. Am. Chem. Soc.*, 2018, **140**, 14753–14760.
114 L. Li, Y. Chen and J. J. Zhu, *Anal. Chem.*, 2017, **89**, 358–371.
115 A. J. Wilson, K. Marchuk and K. A. Willets, *Nano Lett.*, 2015, **15**, 6110–6115.
116 S. Pan, J. Liu and C. M. Hill, *J. Phys. Chem. C*, 2015, **119**, 27095–27097.
117 J. I. Lee, D. Kang, S. H. Kong, H. Gim, I. S. Shin, J. Kim and M. S. Kang, *ACS Appl. Mater. Interfaces*, 2018, **10**, 41562–41569.
118 T. Daimon and E. Nihei, *J. Mater. Chem. C*, 2013, **1**, 2826–2833.
119 U. M. Tefashe, Q. V. Nguyen, F. Lafolet, J. C. Lacroix and R. L. McCreery, *J. Am. Chem. Soc.*, 2017, **139**, 7436–7439.
120 S. Tsuneyasu, T. Ichikawa, K. Nakamura and N. Kobayashi, *ChemElectroChem*, 2017, **4**, 1731–1735.
121 H. Hwang, J. K. Kim and H. C. Moon, *J. Mater. Chem. C*, 2017, **5**, 12513–12519.
122 J. Y. Kim, S. Cheon, H. Lee, J. Y. Oh, J. I. Lee, H. Ryu, Y. H. Kim and C. S. Hwang, *J. Mater. Chem. C*, 2017, **5**, 4214–4218.
123 H. C. Moon, T. P. Lodge and C. D. Frisbie, *J. Am. Chem. Soc.*, 2014, **136**, 3705–3712.
124 M. Alvaro, J. F. Cabeza, A. Corma, A. Corma, H. Garcia and E. Peris, *J. Am. Chem. Soc.*, 2007, **129**, 8074–8075.
125 J. Zhang, J. Zhou, C. Tian, S. Yang, D. Jiang, X. X. Zhang and H. Y. Chen, *Anal. Chem.*, 2017, **89**, 11399–11404.
126 A. B. Nepomnyashchii, G. Kolesov and B. A. Parkinson, *ACS Appl. Mater. Interfaces*, 2013, **5**, 5931–5936.
127 M. J. Zhu, J. B. Pan, Z. Q. Wu, X. Y. Gao, W. Zhao, X. H. Xia, J. J. Xu and H. Y. Chen, *Angew. Chem., Int. Ed.*, 2018, **57**, 4010–4014.
128 H. Qi, Y. H. Chen, C. H. Cheng and A. J. Bard, *J. Am. Chem. Soc.*, 2013, **135**, 9041–9049.